Solid particle erosion wear on plasma Sprayed Mild steel and Copper surface

[1]B. Swain, [2]A. Patnaik, [1]S. K. Bhuyan, [3]K. N. Barik, [4]S. K Sethi, [1]S. Samal, [1]S. C. Mishra, [1]Ajit Behera*

[1]Department of Metallurgical & Materials Engineering
National Institute of Technology, Rourkela, Odisha, India
[2] Department of Mechanical Engineering
C. V. Raman College of Engineering, Bhubaneswar, Odisha, India
[3]Department of Chemical Engineering
Indira Gandhi Institute of Technology, Sarang, Odisha, India
[4]Department of Electronics and Tele-communication
Veer Surendra Sai University of Technology, Odisha, India

*Corresponding Author: enggbiswajit92@gmail.com

Abstract

Structural engineering components in plant made of mild steel and copper are affected by severe erosive wear due to presence of particulates in its surrounding. To protect these costly structural elements, we have taken atmospheric plasma spray process. This process is better for mild steel and copper due to several advance properties such as high temperature stability, coating efficiency, wear and corrosion protection. Coating by this process can be applied onto all suitable base materials with the widest variety of powders. In this investigation we have taken industrial waste like fly-ash, quartz and illmenite powder as coating composite material and deposited on Mild Steel and Copper substrates with different weight proportions and different power levels of the plasma torch. Erosion type and their mechanism extensively investigated using scanning electron microscopy. Erosion properties have been studied using Air Jet erosion test Reg. with Silica erodent. Two significant parameters i.e. Erosion rate and Avg. microhardness have been measured by varying input i.e. power lever, velocity of erodent and time of erosion exposure. It is observed that, maximum erosion occurs at normal impact angle that indicates about brittle erosion condition. Different graphs are being plotted between mass loss-rate versus time period/impact pressure/impact angle, which gives good correlation with surface features observed. Based on these observations artificial neural network (ANN) models are developed to predict the result in various parameter setup.

***Keyword**: Erosion wear, Plasma spray, Mass-loss, Surface Properties.*

1. Introduction

Solid particle erosion is to be expected whenever industrial structural elements and equipment surrounding contains hard particles that results in thinning of components, surface roughening, surface degradation, macroscopic scooping appearance, and reduction in functional life of the structure. Surface degradation by erosion affects the plant economy by increasing operating costs, reducing energy efficiency and reducing functional life [1-2]. Hence, it has been considered as a serious problem for engineering applications that responsible for many failures. Many researchers have been investigated to improve the surface properties by different deposition/thick-coating techniques to obstruct the surface degradation [3-7]. Recently, atmospheric plasma spraying find a wide range of applications ranging from textile mills to even

aerospace applications [8-10]. Atmospheric plasma spray technology has the advantage of being able to process various low-grade minerals to obtain value-added products and to deposit ceramics, metals, and even a combination of these, generating near-homogenous composite coatings with the desired microstructure on a range of substrates without requirement of operation in vacuum condition [11-15].

Fly-ash composite coatings have been widely used in the coatings industry for its superior erosive, sliding and abrasive wear properties. This paper studied about fly-ash+ quartz+ illmenite composite coating composition. We have evaluated the coating microstructures of various fly-ash+ quartz+ illmenite coatings produced from different spraying power level. The objective of our investigation is to explore the erosion wear mechanism of fly-ash+ quartz+ illmenite coatings in detail, and determine how these mechanisms are influenced by the coating microstructure.

2. Experimental Procedure

Homogenized mixture of Fly-ash+ quartz+ illmenite (60:20:20 weight ratios) having 40-100 µm size were plasma sprayed on mild steel and copper substrates (1 inch diameter and 3 mm thickness). Non-transferred arc mode atmospheric plasma spraying operation was done using plasma spray system at the Laser & Plasma Technology Division, BARC, Mumbai. Optimized major parameters were the spray torch, powder supply, powder feeder, plasma gas supply, control console, cooling water and spray booth. The plasma input power was varied from 11 to 21 KW by controlling the gas flow rate and arc current. The powder deposited at spraying angle 90°. The parameter set up used during plasma spray is given in table 1. Erosion wear test of these coatings are investigated by using Air Jet erosion test Reg (As per ASTM G76). For erosion study, only a small area of the sample was exposed to particle erosion, while the rest of the sample was wrapped in polyester tape, which allows impact of particle only in the exposed area (Figure 1). Typically 150-250 µm silica erodents are used. The tests were stopped after a short interval of time to calculate the mass loss. Multiple tests were performed at increasing time from 60 sec to 180 sec with increasing pressure from 1 bar to 2.5 bar and constant stand-of-distance of 65 mm. It is known that hard ceramic coating failure occurs at 90° angle [16]. So for high erosion two impact angle 60° & 90° were taken. The morphology of substrate (before worn and after worn) was studied using JOEL T-330 scanning electron microscope. Schematic diagram of the solid particle erosion test rig is given in Figure 2 and the test parameters of erosion are given in Table 2.

Table 1: Operating parameters during coating deposition of fly-ash+ quartz+ illmenite

Operating parameters	values
Plasma arc current (amp)	260-500
Arc voltage (volt)	40-44
Torch input power(KW)	11,15,18,21
Plasma gas(argon) flow rate(IPM)	28
Secondary gas(N2) flow rate(IPM)	3
Carrier gas(Ar) flow rate(IPM)	12
Powder feed rate (gm/min)	15
Torch to base distance(TBD)(mm)	100

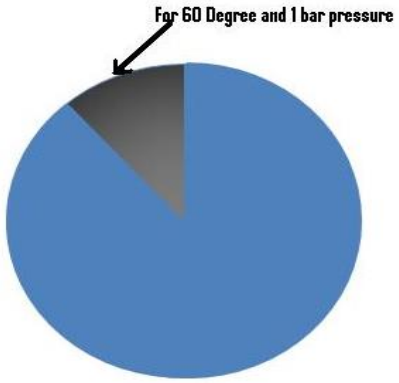

Fig. 1 A small area of fly-ash+ quartz+ illmenite coating exposed for a particular set of experiment.

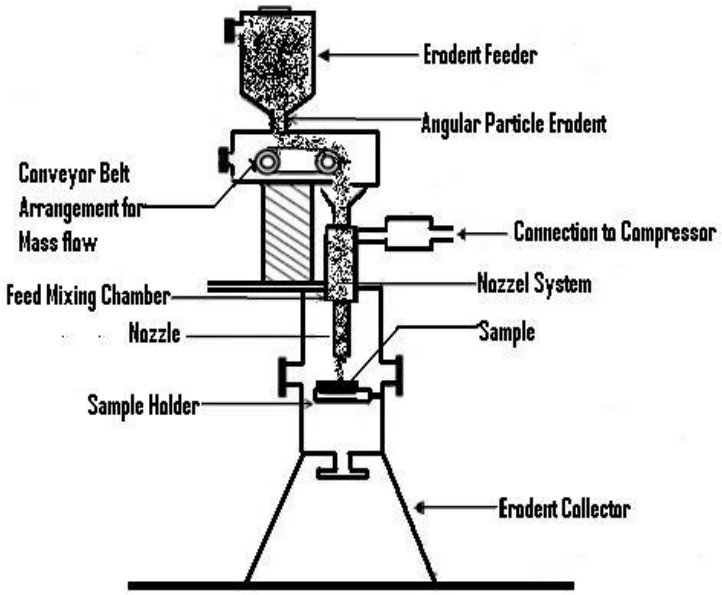

Fig. 2 Schematic diagram of the solid particle erosion test rig.

Table 2: Testing parameter during erosion.

Parameters	values
Testing Temperature	25°C
Impingement Angle	60° & 90°
Erodent impingement pressure	1.0, 1.5, 2.0, 2.5 bar
Test duration	60sec, 120sec & 180sec

.

3. Results and Discussion

3.1 Surface Morphology of eroded fly-ash+quartz+illmenite coatings.

After wear test, all the samples have been examined under SEM. The surface morphology of worn surfaces can be observed from the following four cases.

Case-1: Impacted at an angle 60° & pressure level 1 bar represented in Figure 3(a)

Case-2: Impacted at an angle 60° & pressure level 2 bar represented in Figure 3(b)

Case-3: Impacted at an angle 90° & pressure level 1 bar represented in Figure 3(c)

Case-4: Impacted at an angle 90° & pressure level 2 bar represented in Figure 3(d)

From the above four case it is found that at 60° angle of impact, there are many angular grooves occurs and at 90° angle of impact, sharp vertical groves are seen which is due to dominating effect of perpendicular component of the force of impingement of the erodent. In general it can be stated that when hard and multifaceted erodent i.e. SiC is used, deeper groves are produced and plastically flow regions are found, which limits the surface crack propagation. It is observed that when erodent impact pressure increased, the removal of coating mass increased causing exposure of substrate material. It is also found that when solid particle impingement occurs, groves or craters are formed. Here crater indicates that the particle indenting the region is more rounded, as an angular particle would have cut deeper into the surface creating a more prominent crater-lip [17]. SEM micrograph confirms that the damage mechanism is related to single or multiple splat removal through crack propagation along the splat boundaries of single splat or cluster of splats.

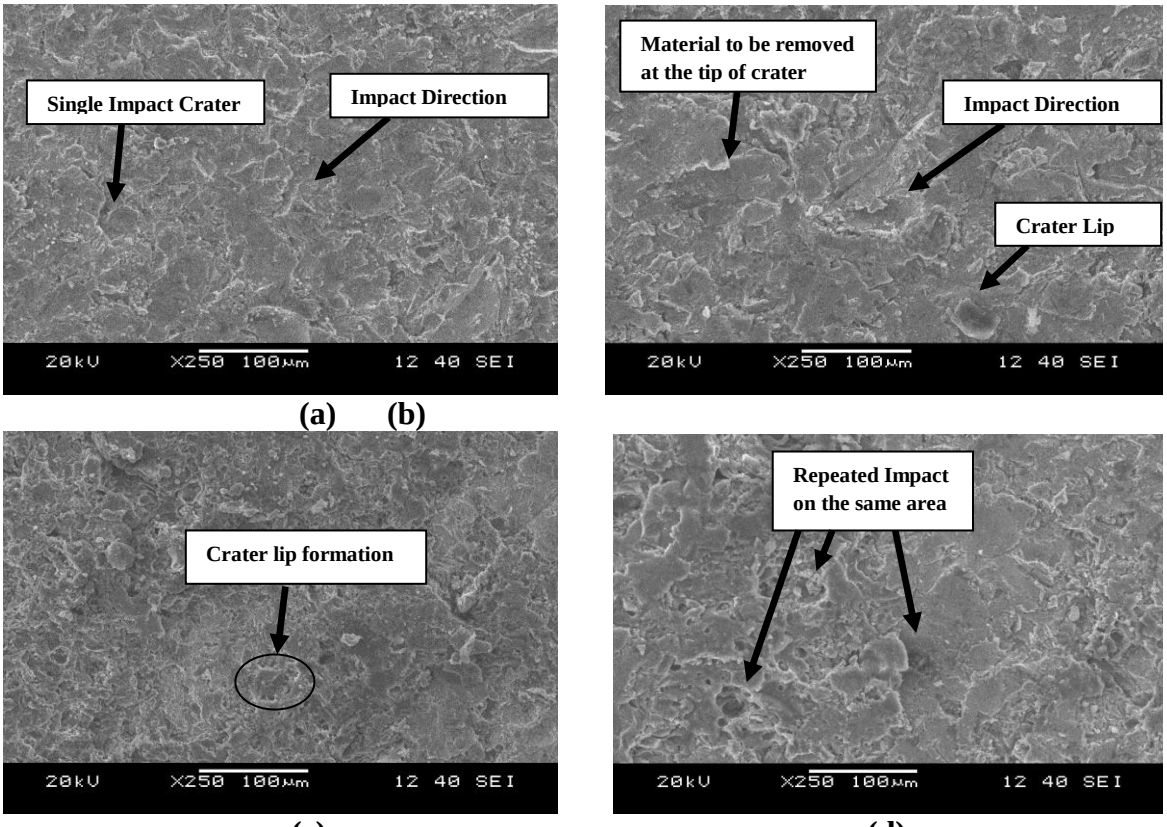

Fig. 3 SEM micrographs of eroded surfaces of coatings deposited at 18 kW, eroded at angle of impact (a) 60° & 1 bar; (b) 60° & 2 bar; (c) 90° & 1 bar; (d) 90° & 2 bar using SiC as the erodent.

3.2 Wear mechanism on fly-ash+ quartz+ illmenite

This wear mechanism based on piled up of material with gradual loss of mass after subsequent impacts by forming crater. Initial piled up material is heavily strained and some small cracks are observed and spread along splats boundaries. This is the reason of fragmentation of splat during solid particle erosion. In Figure 4, it is clearly observed the formation of crater after bombardment of erodent particles on coating surface. Here some of the material would have already been removed as fragmented material (clear boundary shown in Figure 4). For this mechanism the steps may responsible are as follows:

Step 1: There may be two particles of different sizes impact next to each other at same point.

Step 2: Impact of irregular shaped angular particle with different prominent tip/edges during the same impact, can cut more different sites of the surface.

Step 3: Just before subsequent particle impact, a small fragment of the particle breaks off and cuts the adjacent site, which expose for further mass loss.

Step 5: A stream of particles subsequently may impact within the same area.

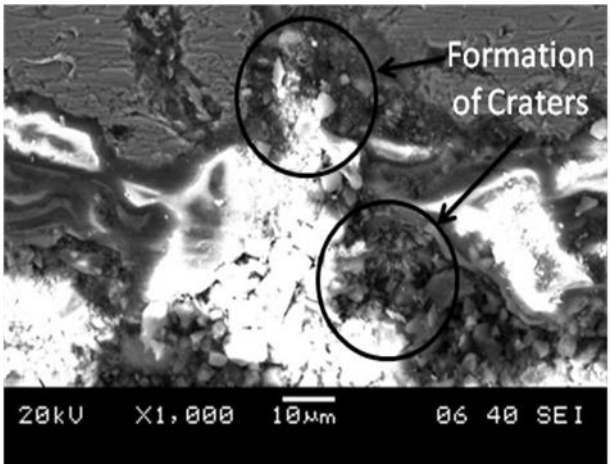

Fig. 4 Typical crater formation on the plasma coating surface.

3.3 Hardness

Table 3 illustrates the micro-hardness and erosion rate profiles of different samples with respect to different experimental condition (in account of power level and impact pressure). It is found that an average hardness is within a range of 532.77 Hv to 659.75 Hv and erosion rate is in the range of 60.1×10^{-4} to 283.74×10^{-4}. This variation arises due to distribution of composite coating and transformation of different phases in the time of specimen preparation (basically due to different power supply for coating). From Table 3, it is clear that, erosion rate increases with increase in impact pressure. Wear behavior of coated composite layers also depend on different powder feed rates and input energy conditions [18]. It is found that, the sample prepared by 18kW power level has greater hardness and less erosion rate for all test conditions.

Table 3: Erosion rate and micro-hardness of different sample at different test conditions.

	Input			Output	
Sl. No.	Power level (kW)	Pressure (bar)	Test Duration (Sec)	Erosion rate$\times10^{-4}$	Avg. Micro-hardness (Hv)
1	11	1.0	60	122.96	532.77
2	11	1.5	60	134.81	537.12

3	11	2.0	60	238.09	534.09
4	11	2.5	60	283.74	536.78
5	11	1.0	120	130.67	530.13
6	11	1.5	120	141.58	537.24
7	11	2.0	120	254.14	532.89
8	11	2.5	120	297.66	534.28
9	11	1.0	180	145.97	531.35
10	11	1.5	180	156.33	535.78
11	11	2.0	180	267.75	533.29
12	11	2.5	180	310.32	536.97
13	15	1.0	60	64.33	566.25
14	15	1.5	60	68.57	573.90
15	15	2.0	60	115.76	576.51
16	15	2.5	60	120.00	582.71
17	15	1.0	120	71.39	568.39
18	15	1.5	120	79.48	574.11
19	15	2.0	120	126.95	575.32
20	15	2.5	120	132.49	583.21
21	15	1.0	180	76.26	567.27
22	15	1.5	180	83.69	576.23
23	15	2.0	180	131.68	575.27
24	15	2.5	180	136.22	782.55
25	18	1.0	60	34.92	653.99
26	18	1.5	60	60.10	659.75
27	18	2.0	60	78.94	642.94
28	18	2.5	60	109.62	653.98
29	18	1.0	120	43.24	654.01
30	18	1.5	120	64.22	661.23
31	18	2.0	120	84.29	645.76
32	18	2.5	120	115.27	659.37
33	18	1.0	180	47.38	659.25
34	18	1.5	180	68.48	662.76
35	18	2.0	180	92.65	646.21
36	18	2.5	180	121.56	659.23
37	21	1.0	60	23.28	590.66
38	21	1.5	60	72.42	590.70
39	21	2.0	60	80.84	590.75
40	21	2.5	60	116.19	590.77
41	21	1.0	120	35.68	590.21

42	21	1.5	120	83.64	593.21
43	21	2.0	120	89.34	592.55
44	21	2.5	120	124.84	594.24
45	21	1.0	180	42.56	592.11
46	21	1.5	180	87.26	593.28
47	21	2.0	180	94.74	593.28
48	21	2.5	180	129.34	596.22

3.4 **XRD Analysis**

Different phases present in specific samples are given in Figure 5 for subsequent spray power level (11 kW, 15 kW, 18 kW and 21 kW respectively). Additionally, the presence of titanium, iron, and silicon compounds in the coating phase greatly increased the hardness. These composite phases were more effective in improving wear resistance.

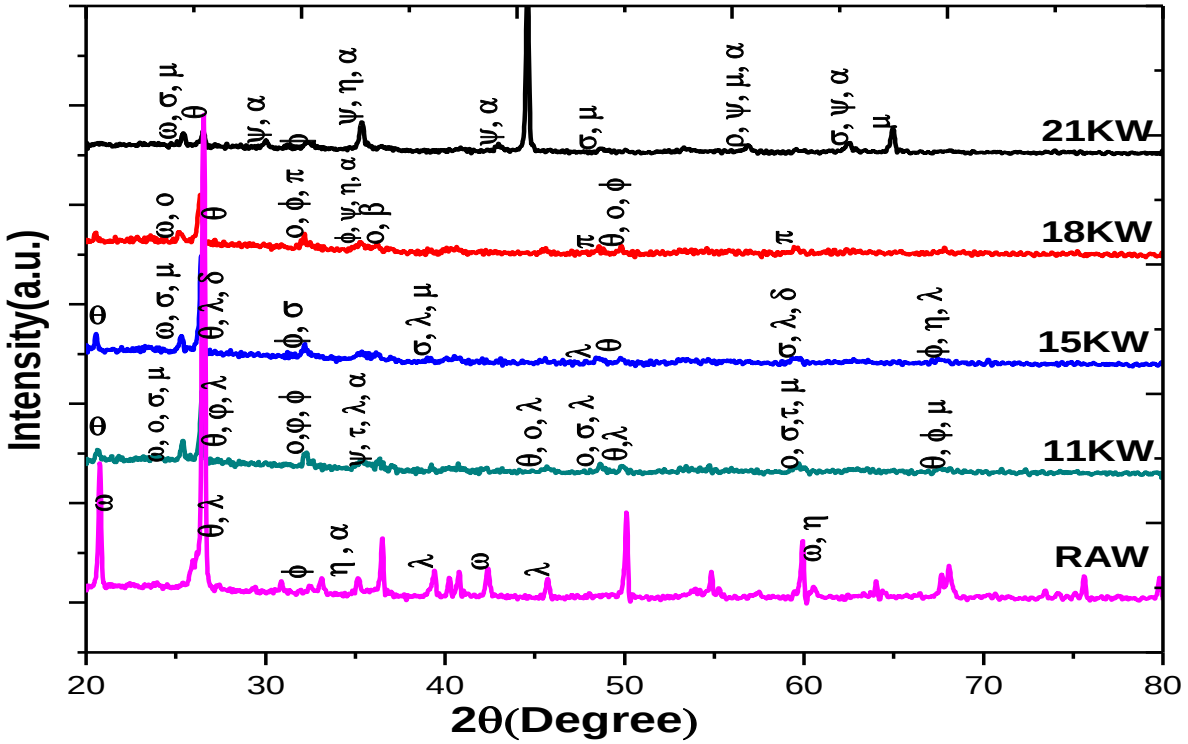

Fig. 5 X-ray diffraction pattern showing different phases present in different sample (Different sample power level are indicated in right side of the pattern)

(Θ=SiO_2, ω=TiO_2, O=Ti_3O_5, φ=Ti_4O_7, ρ=TiO, ε=Ti_2O, Φ =$FeTiO_3$, σ=Fe_2TiO_5, Ψ=Fe_3O_4, ζ=Fe_2O_3, ή=Al_2O_3, λ= Al_2SiO_5, δ=Al_6SiO_{13}, μ=$Fe_2MnTi_3O_{10}$, π=FeSiO, α=$NiMn_2O_4$, β=$MnAl_2O_4$)

Figure 6 shows the graph between erosion rate and micro-hardness of plasma sprayed fly-ash+ quartz+ illmenite coating. Figure indicates erosion rate decreases as increasing in coating hardness. But in some cases, erosion rate becomes little higher as there is increase in hardness as comparison to other. This is due the presence of larger amount of void present in the coating, semi-molten phases etc.

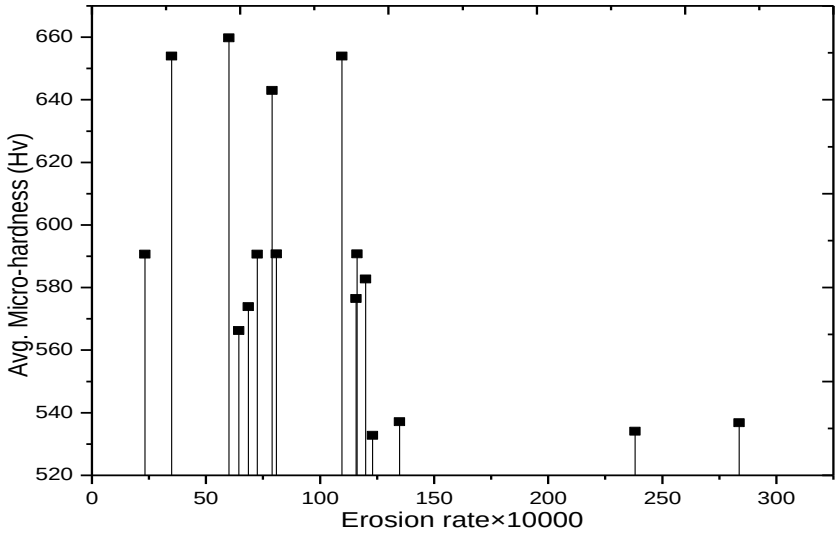

Fig. 6 Erosion Rate Vs micro-hardness of plasma sprayed fly-ash+ quartz+ illmenite coating (Erosion at 90° angle of incident).

3.4 Graphical presentation of coating mass with respect to erosion time

Figure 7 shows that mass of coating sample versus time in order to identify the erosion rate. Here time duration taken from 60 sec to 180 sec. between 60 sec to 120 sec, when particles are impacted on fresh uneroded coating surface, each erodent causes material removal by forming prominent lips and craters [19]. Here it is found that the mass loss increases with increase in time. Mass loss rate can be obtained by the average mass loss at a particular time divided by the time duration. In between 120 sec and 180 sec, in some case, there is decrease in mass loss. This is due to: (a) strain-againg as sticking of the surface materials [20] or (b) the efficiency of erodent retarded due to the rough uneven surface which absorbs the particle impact energy and hinder for mass loss [21] or (c) due to brittle to ductile transition behavior [22]. The variation of mass loss with time, in case of the coating eroded by SiC for 18kW are illustrated in Fig 7(a) & (b) and for 21kW illustrated in Fig 7(c) & (d). From the figures, the mass of the coating material decreases with time period. The initial mass loss is high and it follows a steady state after certain time of exposure. Finnie [23] has explained that the drastic drop of erosion rates is due to transition of type of fracture mechanism i.e. from brittle to ductile behavior. From these figures, it is concluded that the initial wear rate is high irrespective of the angle of impact. With increasing exposure time the rate of wear starts decreasing and in the transient regime, a steady state is attended [24]. It is also found that, maximum erosion occurs at normal impact angle. This behavior is observed in case of brittle materials where the erosion rate continuously increases with increasing impact angle and attains a maximum at normal (90°) impact, in addition under brittle erosion conditions the magnitude of erosion rate is determined only by normal component of impact velocity [25]. Erosion rate can be known by a relationship with respect to change of impact angle (α) as predicted by Lishizhou [26] is as follows:

$$E=A\cos^2 \alpha \sin(m\alpha)+B\sin^2\alpha \qquad (4.3)$$

Where A, B & m are constants. A is equal to zero for typical brittle material and the erosion rate is maximum at normal impact. B is equal to zero for ductile material and erosion rate is maximum within 20°-30° impact angle.

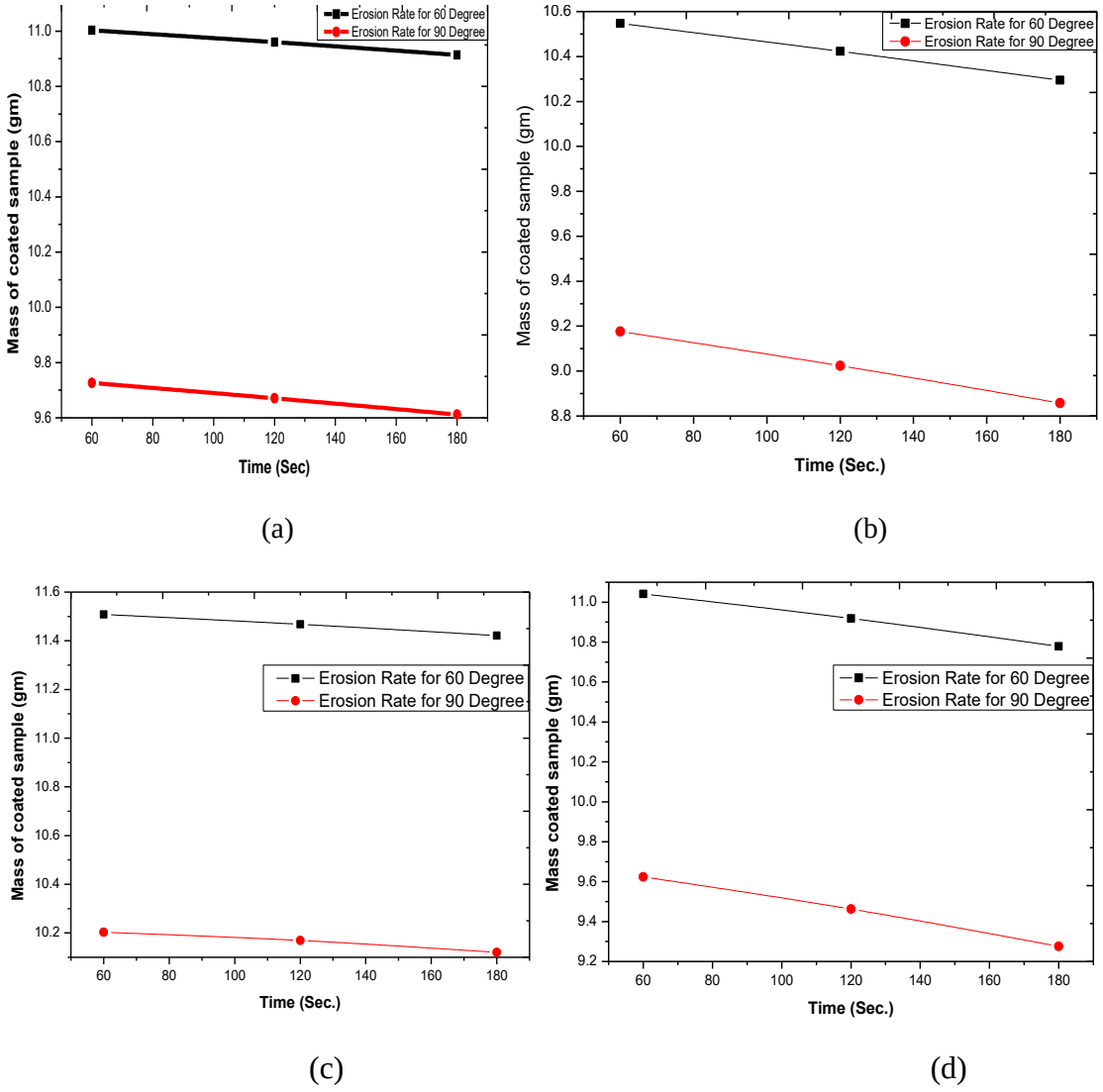

Fig. 7 Coating mass vs time for coating substrate at different power level and erodent impact pressure (a) for 18 kW, 1 bar, (b) for 18 kW, 2 bar; (c) for 21 kW, 1 bar; (d) for 21 kW, 2 bar.

3.5 Analysis of erosion rate with respect to erosion angle

Figure 8 represents the erosion rate w.r.t two angle 60° and 90° of various plasma sprayed sample of different spraying power (11 to 21 KW). It is clear that at lower gun power (60° and 90°), the erosion is more in 90° angle. This is due to presence of larger number of semi-moltel particle. By increasing the power level from 18 to 21 KW, the erosion rate reduces from 60° to 90°. For 21 KW power level plasma sprayed sample, the erosion rate reduces from 116.19 $gm.sec^{-1}$ to 23.28 $gm.sec^{-1}$. So, it is clear that the brittleness of the plasma sprayed sample

decreases with increase in power lever. This is happened due to deposition of fully molten metal at higher gun power.

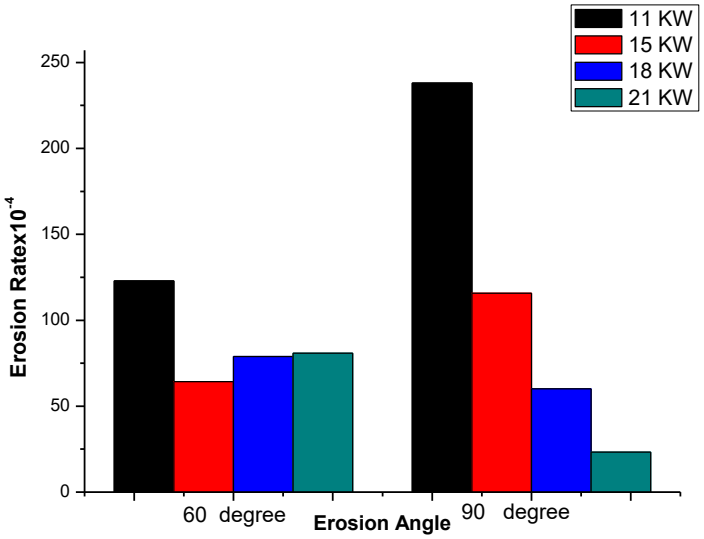

Fig. 8: Erosion rate at different erosion angle.

4 Conclusions

The coating characteristic such as erosion rate and hardness are changed due to phase transformations and semi-molten powder deposition during plasma spraying. The trio-combination like flyash+ quartz+ illmenite coating gives much harder than substrate metals for which it can be recommended for tribological applications. It is clear that erosion wear strongly influence by size of erodent, impact velocity, impact angle standoff distance and hardness etc. Maximum erosion took place at a normal angle of impact. Here it is observed that, this type of erosion mechanism initiate through plastic deformation.

The study of erosion wear behavior is the main requirement for recommending plasma spraying for a specific application. It is concluded that the composite coating materials are more effective for improvement of wear resistance and flyash+ quartz+ illmenite can be considered as a potential coating material suitable for various tribological applications, making a sustainable usage of industrial waste and a progress towards the harness of a green and lively environment.

5 References

[1] B. A. Cook, J.S. Peters, J.L. Harringa, A.M. Russell, Enhanced wear resistance in AlMgB14-TiB_2 composites, Wear 271 (2011) 640-646.

[2] R. Chattopadhyay, Surface Wear: Analysis, Treatment, Prevention, vols. Xi-xii, ASM International, Materials Park, OH, USA (2001) 267-290.

[3] Mustafa Ulutan, M. Mustafa Yildirim, Soner Buytoz, and Osmann. C Elik, “Microstructure and Wear Behavior of TIG Surface-Alloyed AISI 4140 Steel”, Tribology Transactions, 54: (2011) 67-79, DOI: 10.1080/10402004.2010.519859.

[4] Suvendu pr. Sahu , Alok Satapathy, Debadutta Mishra, Amar Patnaik & K. P.Sreekumar, Tribo-Performance Analysis of Fly Ash-Aluminum Coatings Using Experimental Design and ANN, Tribology Transactions, 53: (2010) 533-542, DOI: 10.1080/10402000903491317.

[5] M. Toparli, E. Celik, I. Birlik, E. Dokumaci & N. F. Ak Azem, Tribological Properties of Electric Arc–Sprayed CuSn Coating for Bearing Elements, Tribology Transactions, 52: (2009) 389-394, DOI: 10.1080/10402000802593122.

[6] Y. Y. O Zbek, M. Durman, and H. Akbulut, Wear Behavior of AISI 8620 Steel Modified by a Pulse-Plasma Technique, Tribology Transactions, 52: (2009) 213-222, DOI: 10.1080/10402000802369721.
[7] S. C. Mishra, Anupama Sahu, Rojaleen Das, Alok Satapathy and S. Sen, Microstructure, Adhesion and Erosion wear of plasma sprayed Alumina-Titania composite coatings, Journal of Reinforced Plastics and Composites, Vol. 00 (2008) 1-11.
[8] P. Louda, S. Tumova, Z. Rozek, Application of nanotechnology at automotive industry, In International Conference Vacuum and Plasma Surface Engineering, Liberec, Technical University of Liberec (2006) ISBN 80-7372-129-5.
[9] S. C. Mishra, S. Das, A. Satapathy, S. Sarkar, P. V. Ananthapadmanabhan, K. P. Sreekumar, "Investigation on Composite Coating of Low Grade Minerals," Journal of Reinforced Plastics and Composites, 24 (2009) 3061-3067.
[10] Alok Satapathy, Suvendu Prasad Sahu, Debadutta Mishra, Development of protective coatings using fly ash, premixed with metal powder on aluminium substrates, Waste Management & Research, (2009) 1-7.
[11] Ajit Behera, S.C. Mishra, Dependence of Adhesion Strength of Plasma Spray on Coating Surface Properties, journal of materials and metallurgical and engineering, Vol. 2, Issue 1 (2012) 23-30.
[12] H. W. Grunling And W. Mannsmann, Plasma sprayed thermal barrier coatings for industrial gas turbines: morphology, processing and properties, Journal De Physique IV, Colloque C7, supplkment au Journal de Physique 111, Vol. 3 (1993) 903-912.
[13] Mark F. Smith, Aaron C. Hall, James D. Fleetwood and Philip Meyer, Coatings, 1 (2011) 117-132; doi:10.3390/coatings1020117.
[14] Y. C. Tsui, C. Doyle, T.W. Clyne, Plasma sprayed hydroxyapatite coatings on titanium substrates Part 1: Mechanical properties and residual stress levels, Biomaterials 19 (1998) 2015-2029.
[15] Anand A. Kulkarni, Allen Goland, Herbert Herman, Andrew J. Allen, Jan Ilavsky, Gabrielle G. Long, and Francesco De Carlo, Advanced Microstructural Characterization of Plasma-Sprayed Zirconia Coatings Over Extended Length Scales, Journal of Thermal Spray Technology, Vol. 14(2) (2005) 239-250.
[16] Jose Roberto Tavares Branco, Robert Gansert, Sanjay Sampath, Christopher C. Berndt, Herbert Herman, Solid Particle Erosion of Plasma Sprayed Ceramic Coatings, Materials Research, Vol. 7, No. 1 (2004)147-153.
[17] S. S. Rajahramn, T. J. Harvey, J.C. Walker, S.C. Wang, R.J.K. Wood, "Investigation of erosion-corrosion mechanisms of UNS S31603 using FIB and TEM", Tribology International 46 (2012) 161-173.
[18] Serdar Osman Yılmaz, Wearbehavior of gas tungsten arc deposited FeCrC, FeCrSi, and WCo coatings on AISI 1018 steel, Surface and Coatings Technology, Vol. 194, Issues 2-3 (2005) 175-183.
[19] R. L. Howard, A. Ball, The solid particle and cavitation erosion of titanium aluminide intermetallic alloys, Wear, Vol. 186-187, Part 1 (1995) 123-128.
[20] C. S. Ramesh, R. Keshavamurthy, B. H. Channabasappa, S. Pramod, Influence of heat treatment on slurry erosive wear resistance of Al6061 alloy, Materials and Design 30 (2009) 3713-3722.
[21] J. R. Davis, Surface Engineering for corrosion and wear resistance, ASM International, ISBN: 0-87170-700-4.

[22] N. M. Barkoula, J. Gremmels, J. Karger-Kocsis, Dependence of solid particle erosion on the cross-link density in an epoxy resin modified by hygrothermally decomposed polyurethane, Wear 247 (2001) 100-108.
[23] S. C. Mishra, S. Praharaj, Alok Satpathy, Evaluation of Erosion Wear of A Ceramic Coating With Taguchi Approach, Journal of Manufacturing Engineering, Vol.4, Issue.2 (2009) 241-246.
[24] A. J. Sparks, I.M. Hutchings, "Transitions in Erosive Wear behavior of Glass Ceramic", Wear, Vol. 149 (1991) 99-110.
[25] Ajit Behera, M.Tech Thesis, "Processing and characterization of plasma spray coatings of industrial waste and low grade ore mineral on metal substrates" submitted In Department of Metallurgical & Materials Engineering, National Institute of Technology, Rourkela, India, 2012.
[26] Yi Maozhong, Huang Baiyun, He Jiawen, Erosion wear behaviour and model of abradable seal coating, Wear 252 (2002) 9-15.